Recent Results in Trapped-Ion Quantum Computing at NIST

D. Kielpinski, A. Ben-Kish, J. Britton, V. Meyer, M.A. Rowe, C.A. Sackett[1], W.M. Itano, C. Monroe[2], and D.J. Wineland

Time and Frequency Division, National Institute of Standards and Technology, Mailstop 847, 325 Broadway, Boulder CO 80303, USA

E-mail: davidk@boulder.nist.gov

[1] *Department of Physics, University of Virginia, Charlottesville VA 22904, USA*

[2] *Department of Physics, University of Michigan, Ann Arbor MI 48109, USA*

arXiv:quant-ph/0102086v1 16 Feb 2001

We review recent experiments on entanglement, Bell's inequality, and decoherence-free subspaces in a quantum register of trapped $^9Be^+$ ions. We have demonstrated entanglement of up to four ions [1] using the technique of Mølmer and Sørensen [2]. This method produces the state $(|\uparrow\uparrow\rangle+|\downarrow\downarrow\rangle)/\sqrt{2}$ for two ions and the state $(|\downarrow\downarrow\downarrow\downarrow\rangle + |\uparrow\uparrow\uparrow\uparrow\rangle)/\sqrt{2}$ for four ions. We generate the entanglement deterministically in each shot of the experiment. Measurements on the two-ion entangled state violates Bell's inequality at the 8σ level [3]. Because of the high detector efficiency of our apparatus, this experiment closes the detector loophole for Bell's inequality measurements for the first time. This measurement is also the first violation of Bell's inequality by massive particles that does not implicitly assume results from quantum mechanics. Finally, we have demonstrated reversible encoding of an arbitrary qubit, originally contained in one ion, into a decoherence-free subspace (DFS) of two ions [4]. The DFS-encoded qubit resists applied collective dephasing noise and retains coherence under ambient conditions 3.6 times longer than does an unencoded qubit. The encoding method, which uses single-ion gates and the two-ion entangling gate, demonstrates all the elements required for two-qubit universal quantum logic.

I. INTRODUCTION

Trapped ions are a promising candidate system for implementing quantum computing (QC), with potential applications like efficient factorization of large numbers [5] and efficient searching of large databases [6]. While large-scale QC is still far off, trapped-ion quantum registers have already demonstrated all the essential ingredients of QC, including initialization to a known quantum state [7,8,10], efficient detection of final states [3,10], long qubit coherence times [4,11–13], and a universal set of quantum logic gates [1,10,14,15]. Recent work on trapped-ion QC at NIST has used this basic set of tools to produce four-particle entanglement [1], observe violation of Bell's inequality [3], and encode quantum information into a decoherence-free subspace [4].

In the experiments described below, the qubits are electronic states of $^9Be^+$ ions held in a linear RF trap [16] of the type described in reference [17]. The relevant electronic energy levels of the $^9Be^+$ ion are shown in Fig. 1. Each ion encodes one qubit in its $^2S_{1/2}|F=2,m_F=-2\rangle$ and $^2S_{1/2}|F=1,m_F=-1\rangle$ hyperfine sublevels, denoted by $|\downarrow\rangle$ and $|\uparrow\rangle$, respectively. The ions are readily initialized in $|\downarrow\rangle$ by optical pumping. We detect the number of ions in state $|\downarrow\rangle$ by applying left circularly polarized laser light to excite the $|\downarrow\rangle$ - $^2P_{3/2}$ transition at about 313 nm. The polarization of the light ensures excitation to the $^2P_{3/2}|F=3,m_F=-3\rangle$ hyperfine sublevel, which can only decay to the $|\downarrow\rangle$ sublevel by dipole selection rules. Thus an ion in state $|\downarrow\rangle$ can scatter thousands of photons without changing its hyperfine state. On the other hand, state $|\uparrow\rangle$ is spectrally resolved from $|\downarrow\rangle$ by the hyperfine splitting of 1.25 GHz and therefore scatters very little light. The resulting detection accuracy per ion is about 98% in a single shot of the experiment.

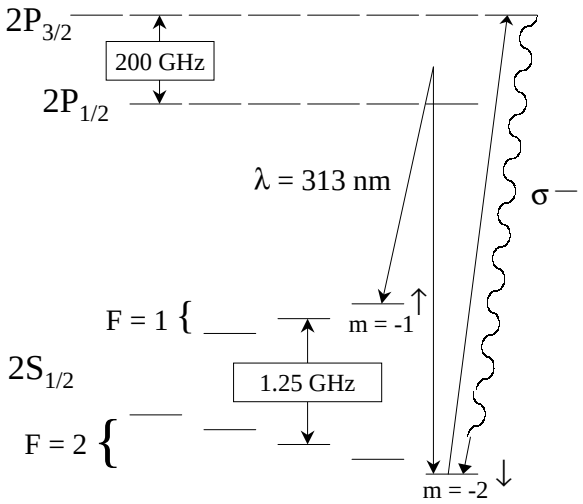

FIG. 1. Partial level diagram of the $^9Be^+$ ion, showing the cycling transition for σ_- resonant light and the two-photon off-resonant coupling for Raman transitions. Wavelengths for all transitions are approximately 313 nm.

We produce controlled rotations of a single qubit by

driving stimulated Raman transitions between states $|\uparrow\rangle$ and $|\downarrow\rangle$. The laser beams driving the transitions are tuned about midway between the $^2P_{3/2}$ and $^2P_{1/2}$ states. If the frequency difference $\nu_{\rm diff}$ between the Raman laser beams is equal to the energy splitting ν_0 between states $|\uparrow\rangle$ and $|\downarrow\rangle$, we observe Rabi flopping between $|\uparrow\rangle$ and $|\downarrow\rangle$ corresponding to the evolution

$$|\downarrow\rangle \rightarrow \cos\frac{\theta}{2}|\downarrow\rangle + e^{i\phi}\sin\frac{\theta}{2}|\uparrow\rangle \qquad (1)$$
$$|\uparrow\rangle \rightarrow \cos\frac{\theta}{2}|\uparrow\rangle - e^{-i\phi}\sin\frac{\theta}{2}|\downarrow\rangle$$

Here θ is proportional to the Raman pulse duration and ϕ is the phase difference between the Raman beams at the position of the ion, referred to as the "ion phase". For two ions, we write the ion phases as ϕ_1, ϕ_2. We can effect common-mode changes of ϕ_1 and ϕ_2 by changing the phase of the RF synthesizer that controls the Raman difference frequency. By changing the strength of the trap, we can control the ion spacing precisely, allowing us to make differential changes to ϕ_1 and ϕ_2. These two techniques combined allow us to control ϕ_1 and ϕ_2 independently for two ions, so that we can perform single-qubit rotations on one ion without affecting the other [4].

The potential created by the ion trap is harmonic with axial frequency $\nu_{\rm CM}$ of about 5 MHz. Doppler cooling allows us to cool the ions to temperatures $T \sim h\nu_{\rm CM}/k_B$. The Doppler-cooled ions are strongly coupled by the Coulomb interaction and form a rigid crystal, which in these experiments is a string of ions lying along the trap axis. Because the ions are strongly coupled, their quantized motion is best described in terms of normal modes with frequencies ν_i. For two ions, for instance, the motion of the ions along the axis decomposes into symmetric and antisymmetric normal modes at frequencies $\nu_{\rm CM}$ and $\sqrt{3}\nu_{\rm CM}$. The lowest-lying normal mode for any number of ions is the center-of-mass mode at frequency $\nu_{\rm CM}$. In this mode the ion string moves as a unit.

We can control the motional quantum state of the ions by driving stimulated Raman transitions that couple spin and motion. In our geometry, the wavevector difference between Raman beams lies along the axis of the ion trap, so the Raman beams exert a dipole force only along the axis. Setting $\nu_{\rm diff}$ equal to $\nu_0 + m\nu_i$ (m an integer) induces Rabi flopping between states $|\downarrow\rangle|n\rangle$ and $|\uparrow\rangle|n+m\rangle$ with evolution like that of Eq. (1). Here $|n\rangle$ denotes the nth Fock state of the ith normal mode. In particular, we can cool the ions by driving a pulse with $\theta = \pi$ at $\nu_{\rm diff} = \nu_0 - \nu_i$ (the "red sideband") and optically pumping from $|\uparrow\rangle$ back to $|\downarrow\rangle$. Repeating the cycle several times permits preparation of the ion string in its motional ground state [7,8].

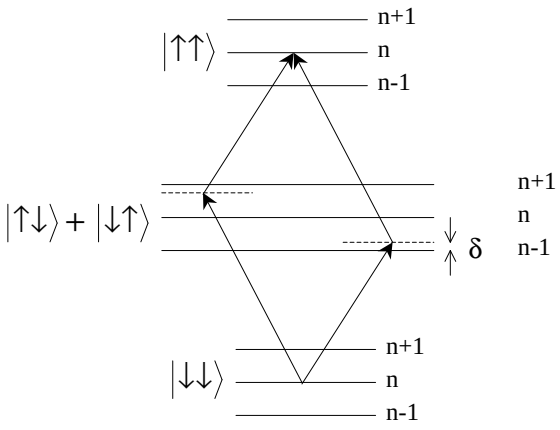

FIG. 2. Level diagram for the Sørensen-Mølmer entangling gate in the case of two ions. Here, as opposed to Fig. 1, arrows indicate two-photon Raman transitions. Raman transitions near both red and blue sidebands are applied simultaneously to create the state $(|\downarrow\downarrow\rangle + |\uparrow\uparrow\rangle)/\sqrt{2}$.

II. GENERATING ENTANGLEMENT

We have entangled strings of up to four ions [1] using the technique proposed by Sørensen and Mølmer [2]. In this method, one drives two Raman transitions simultaneously, with the same Rabi frequency on all ions. Fig. 2 shows an energy-level diagram including the relevant transitions. The detuning δ ensures that population transfer between motional states is nonresonant and therefore small. However, the sum of the two Raman transition frequencies is $2\nu_{\uparrow\downarrow}$, so that for any pair of ions the process $|\downarrow\downarrow\rangle \leftrightarrow |\uparrow\uparrow\rangle$ is resonant. For N ions initially in $|\downarrow\rangle$, the resulting evolution produces the state

$$|\psi_e\rangle = \begin{array}{ll} (|\downarrow\downarrow\rangle + |\uparrow\uparrow\rangle)/\sqrt{2} & \text{(two ions)} \\ (|\downarrow\downarrow\downarrow\downarrow\rangle + |\uparrow\uparrow\uparrow\uparrow\rangle)/\sqrt{2} & \text{(four ions)} \end{array} \qquad (2)$$

both of which are maximally entangled states.

To implement this technique, we pass one of the Raman beams through an electro-optic modulator (EOM) to generate the two required Raman difference frequencies and uniformly illuminate the ion string with both Raman beams. For two ions, we tune the Raman difference frequencies close to the motional sidebands of the antisymmetric mode; for four ions, we use the mode with frequency $\sqrt{29/5}\ \nu_{\rm CM}$. In both cases, the mode we choose has equal amplitudes of motion for all ions, so that the Raman Rabi frequencies for all ions are the same under uniform illumination.

In general, the state produced by this method is characterized by some density matrix ρ that approximates the desired state $|\psi_e\rangle$. To show entanglement of the experimental state ρ, it is sufficient to show that the fidelity $F = \langle\psi_e|\rho|\psi_e\rangle$ exceeds 1/2 [1,9]. We have

$$F = (\rho_{\downarrow\downarrow\ldots\downarrow\downarrow} + \rho_{\uparrow\uparrow\ldots\uparrow\uparrow})/2 + |\rho_{\downarrow\downarrow\ldots\uparrow\uparrow}| \quad (3)$$

We measure the diagonal density matrix elements $\rho_{\downarrow\ldots\downarrow,\downarrow\ldots\downarrow}, \rho_{\uparrow\ldots\uparrow,\uparrow\ldots\uparrow}$ by detecting the number of ions in $|\downarrow\rangle$. To find the far-off-diagonal coherence $|\rho_{\downarrow\ldots\downarrow\uparrow\ldots\uparrow}|$, we rotate all ions together as in Eq. (1) with $\theta = \pi/2$ and with phases $\phi_i = \phi$ relative to the entangling pulse. Then we measure the parity Π of the ion string, defined as $+1$ for an even number of ions in $|\downarrow\rangle$, -1 for an odd number in $|\downarrow\rangle$. It is easy to show that

$$\Pi = 2|\rho_{\downarrow\downarrow\ldots\uparrow\uparrow}| \cos N\phi \quad (4)$$

for N ions, if all other off-diagonal coherences are absent. Sweeping the phase of the RF synthesizer that generates the Raman difference frequency gives a sinusoidal signal of Π vs. ϕ, as shown in Fig. 3. We extract the coherence $|\rho_{\downarrow\downarrow\ldots\uparrow\uparrow}|$ by fitting a sine wave to the data of Fig. 3. The density matrix elements needed to calculate the fidelity are given in Table 1 for two and four ions. For two ions we find $F = 0.83 \pm 0.01$, while for four ions $F = 0.57 \pm 0.02$, demonstrating entanglement in both cases [1]. It is important to note that the data used to calculate F are not post-selected. Since the evolution is deterministic, our method produces an entangled state in each shot of the experiment.

TABLE I. Partial density matrix of the state produced by the entangling pulse. From Eq. (3), only these matrix elements are needed to determine whether the experimentally generated state is entangled. Errors are ± 0.01 for two ions and ± 0.02 for four ions.

Number of Ions	$\rho_{\downarrow\downarrow\ldots\downarrow\downarrow}$	$\rho_{\uparrow\uparrow\ldots\uparrow\uparrow}$	$\lvert\rho_{\downarrow\downarrow\ldots\uparrow\uparrow}\rvert$
2	0.46	0.385	0.43
4	0.35	0.35	0.215

III. VIOLATION OF A BELL INEQUALITY

Classical physics obeys the principle of local realism, which states that objects have definite properties whether or not they are measured and that measurements of an object's properties are not affected by events taking place sufficiently far away. As shown by Einstein, Podolsky, and Rosen [18], quantum mechanics is incomplete if we assume local realism. Bell [19] proved that quantum mechanics is actually inconsistent with local realism. Quantitative conditions for falsifying local realism by experimental measurements were first proposed by Bell [19] and were developed further by Clauser, Horne, Shimony, and Holt (CHSH) [20]. In such an experiment, one prepares a pair of particles in a repeatable way, subjects them to independent classical manipulations parametrized by variables Φ_1, Φ_2, and measures a classical property yielding a value $P_1(\Phi_1), P_2(\Phi_2) = \pm 1$ for each particle. Defining the correlation function $q(\Phi_1, \Phi_2) = P_1(\Phi_1)P_2(\Phi_2)$, one finds that the Bell inequality

$$B(\alpha_1, \delta_1, \beta_2, \gamma_2) = |q(\delta_1, \gamma_2) - q(\alpha_1, \gamma_2)| + |q(\delta_1, \beta_2) + q(\alpha_1, \beta_2)| \leq 2 \quad (5)$$

holds for any values α_1, δ_1 (resp. β_2, γ_2) of Φ_1 (resp. Φ_2) under the assumption of local realism.

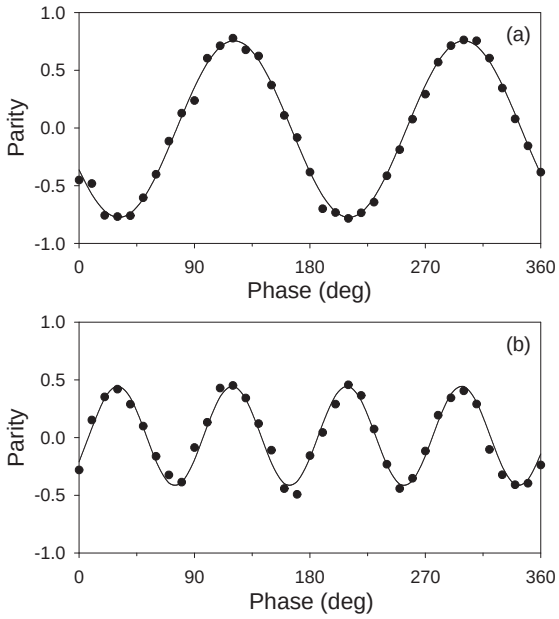

FIG. 3. Measurements of the parity Π as a function of RF synthesizer phase ϕ for two and four ions. The data show clear sinusoidal dependence as in Eq. (4), allowing us to extract the far-off-diagonal coherence $|\rho_{\downarrow\downarrow\ldots\uparrow\uparrow}|$.

In our experiment [3], we apply the entangling operation of Eq. (2) to two ions to prepare our initial state. Then we perform a carrier rotation as in Eq. (1) with $\theta = \pi/2$ and phases ϕ_1, ϕ_2 relative to the entangling pulse phases. Finally, we detect the number of bright ions. The calibration of ϕ_1 and ϕ_2 against the trap strength and the RF synthesizer phase were performed using assumptions from classical physics only [3]. We can therefore identify ϕ_1, ϕ_2 with the classical control parameters Φ_1, Φ_2,

so the experiment is of the type proposed by Bell and CHSH. Quantum mechanics predicts that, for an ideal realization of our experiment, $B(\alpha_1, \delta_1, \beta_2, \gamma_2)$ attains a maximum value of $2\sqrt{2}$ for

$$\begin{array}{rclrcl} \alpha_1 & = & -\pi/8 & \delta_1 & = & 3\pi/8 \\ \beta_2 & = & -\pi/8 & \gamma_2 & = & 3\pi/8 \end{array} \tag{6}$$

contradicting the bound $B(\alpha_1, \delta_1, \beta_2, \gamma_2) \leq 2$ required by local realism.

We repeated the experiment $N_{\rm tot} = 20\ 000$ times for each of the four sets of phases given by Eq. (6). These data are presented as histograms in Fig. 4. We see that the three cases of zero, one, and two ions bright are readily distinguishable. The overlap of histograms corresponding to the three cases gives an inaccuracy of 2% in discriminating between the three cases. This inaccuracy mostly arises from pumping of the $|\downarrow\rangle$ state to the $|\uparrow\rangle$ state because of imperfect polarization of the detection light. Counting the number of events N_0 (N_1, N_2) with zero (one, two) ions bright, we extract the correlation function using

$$q = \frac{(N_0 + N_2) - N_1}{N_{\rm tot}} \tag{7}$$

and obtain a set of four values of $q(\phi_1, \phi_2)$. We repeated the entire procedure five times to ensure that the measured Bell signal did not vary significantly from run to run. The five sets of correlation functions and the resulting Bell signals are shown in Table 2. The statistical error of each Bell signal was ± 0.01. Averaging the Bell signals together, we find

$$B(-\frac{\pi}{8}, \frac{3\pi}{8}, -\frac{\pi}{8}, \frac{3\pi}{8}) = 2.25 \pm 0.03 \tag{8}$$

an 8σ violation of the Bell inequality Eq. (5). The error in the average Bell signal significantly exceeds the error of each individual measurement of the Bell signal. This discrepancy arises from errors in setting the phases of Eq. (6).

This experiment gives the first violation of the Bell inequality for massive particles obtained using a complete set of correlation measurements. A previous experiment [21] deduced a violation from an incomplete set of measurements. Furthermore, our data uses the outcome of every shot of the experiment, so the violation is obtained without the use of the fair-sampling hypothesis. In principle, sampling or post-selection of the data allows violation of Eq. (5) even by local hidden-variable theories, the so-called "detector loophole" [22]. Our experiment closes the detector loophole for the first time. However, the "locality loophole" [23] remains open for our data; since the detection events on the two ions occur within each other's lightcones, in principle the detections could influence each other, leading to spurious correlations.

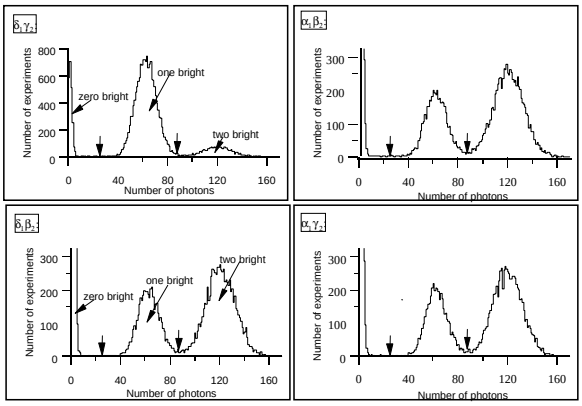

FIG. 4. Histograms of fluorescence signals for the four sets of phases given in Eq. (6). The vertical arrows break up the data into cases of zero, one, or two ions bright with 98% accuracy.

TABLE II. The correlation values and resulting Bell's signals for five runs of the experiment. The phase angles $\alpha_1, \delta_1, \beta_2, \gamma_2$ are given by Eq. (6). The statistical errors are 0.006 and 0.012 for the values of q and B respectively.

$q(\alpha_1, \beta_2)$	$q(\alpha_1, \gamma_2)$	$q(\delta_1, \beta_2)$	$q(\delta_1, \gamma_2)$	$B(\alpha_1, \delta_1, \beta_2, \gamma_2)$
0.541	0.539	0.569	-0.573	2.222
0.575	0.570	0.530	-0.600	2.275
0.551	0.634	0.590	-0.487	2.262
0.575	0.561	0.559	-0.551	2.246
0.541	0.596	0.537	-0.571	2.245

IV. ENCODING INTO A DECOHERENCE-FREE SUBSPACE

Information stored in a quantum system is liable to be lost through coupling of the system to its environment, a process called decoherence [24,25]. In particular, many proposed quantum computer implementations decohere through a mechanism that couples each qubit to the environment equally strongly [26,27]. Encoding quantum information into a decoherence-free subspace (DFS) [28–30] whose states are invariant under coupling to the environment allows information storage even in the presence of this type of decoherence. We have demonstrated the immunity of a DFS of two atoms to environment-induced dephasing and implemented a technique for encoding an arbitrary physical qubit state into the DFS.

The type of decoherence considered here is collective dephasing, in which each qubit undergoes the transformation $|\downarrow\rangle \rightarrow |\downarrow\rangle, |\uparrow\rangle \rightarrow e^{i\zeta}|\uparrow\rangle$ for ζ an unknown phase that is the same from qubit to qubit. One can construct a DFS of two qubits that protects against collective dephasing from the basis states $|\uparrow\downarrow\rangle, |\downarrow\uparrow\rangle$. Any superposition of these states is clearly invariant under collective dephasing, and since there are two states, we can encode one "logical qubit" in this subspace of the two "physical qubits". To demonstrate our encoding technique, we first prepare a state of form

$$|\downarrow\rangle(a|\downarrow\rangle + b|\uparrow\rangle) \qquad |a|^2 + |b|^2 = 1 \qquad a, b \text{ complex} \qquad (9)$$

where one of the two physical qubits initially contains the quantum information. In general, we can prepare this state by driving the carrier transition of Eq. (1) on both ions simultaneously, once with $\theta = \beta$, and again with $\theta = \beta$ and ϕ_1 shifted by π. We set $\phi_2 = \alpha$ for both pulses. The final state has $a = \cos 2\beta, b = e^{i\alpha} \sin 2\beta$.

We encode the state of Eq. (9) into the DFS in two steps. First we apply the inverse of the entangling gate, yielding $a(|\downarrow\downarrow\rangle - i|\uparrow\uparrow\rangle) + b(|\downarrow\uparrow\rangle - i|\uparrow\downarrow\rangle)$. Then we drive the carrier with $\theta = \pi/4, \phi_1 = \pi/2, \phi_2 = 0$ to obtain $|\psi_{\rm DFS}\rangle = a(|\downarrow\uparrow\rangle + i|\uparrow\downarrow\rangle) + b(|\downarrow\uparrow\rangle - i|\uparrow\downarrow\rangle)$. The information stored in the physical qubit of ion 2 is now encoded in the logical qubit of the DFS. In the experiment we take $|a| = |b|$, though our method permits preparation and encoding of any state of the more general form.

To read out the encoded information, we reverse the carrier pulse in the encoding and apply the entangling gate to decode $|\psi_{\rm DFS}\rangle$ into $|\downarrow\rangle(a|\downarrow\rangle + b|\uparrow\rangle)$. After decoding, we rotate ion 2 as in preparing the state of Eq. (9) but with the phase on ion 2 changed to α'. We then measure the probability P_2 of finding both ions in $|\downarrow\rangle$. P_2 varies sinusoidally with $\alpha - \alpha'$, and the magnitude of oscillation is equal to the coherence, C, of ion 2. Since we set $|a| = |b| = 1/\sqrt{2}$, ideally $C = 1$. Departures from $C = 1$ measure the effects of both decoherence and imperfect logic. We verified that C is independent of α, thus showing that our encoding method works even if we have no information about the phase of the input state.

To study the effects of decoherence on the DFS-encoded state, we engineered a collective dephasing environment using an off-resonant laser beam with a randomly varying intensity. The beam induces shifts of ν_0 that are common to both ions through the AC Stark effect. The DFS state should resist the dephasing effect of this environment. The coherence of ion 2 in the test state $|\downarrow\rangle(|\downarrow\rangle + e^{i\phi}|\uparrow\rangle)/\sqrt{2}$, however, should be sensitive to collective dephasing. We measure the decay of the test state by simply turning off the encoding and decoding sequences in the procedure used to measure the decay of the DFS-encoded state. We applied the noise beam to the test state and encoded state during a delay time of about 25 μs, as shown in Fig. 5. The coherence without applied noise is about 0.69 for the test state and about 0.43 for the encoded state; they depart from 1 because of imperfect logic gates and detection. For white-noise intensity fluctuations of the Stark-shifting beam, we expect C to decay exponentially for the test state, as shown by the fit line. We also fit the coherence of the DFS state to an exponential decay for comparison. The decay rate of the test state is $0.18(1)\,\mu{\rm s}^{-1}$, while the decay rate of the DFS state is $0.0035(50)\,\mu{\rm s}^{-1}$, consistent with zero decay.

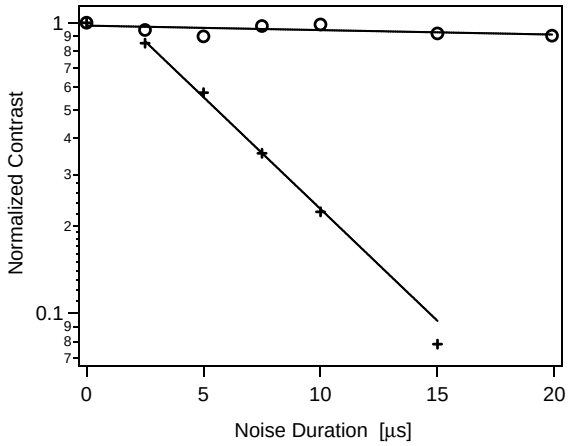

FIG. 5. Decay of DFS-encoded state (circles) and test state (crosses) under engineered dephasing noise. The noise is applied for a fraction of the delay time of about 25 μs between encoding and decoding. Coherence data are normalized to their values for zero applied noise. The fit lines are exponential decay curves. The DFS data is fit for comparison.

We have also measured the storage times of the encoded and test states under ambient conditions in our laboratory. The data are shown in Fig. 6. Here we leave a variable delay time between encoding and decoding to give the ambient noise time to act. The decoherence of the test state is dominated by ambient fluctuating magnetic fields whose frequencies lie primarily at 60 Hz and its harmonics. These fields randomly shift ω_0 through the Zeeman effect. Since these fields are roughly uniform across the ion string, they induce collective dephasing similar to that created by the engineered environment. We empirically find the decay of both test and encoded states to be roughly exponential, as indicated by the fit lines. The decay rate of the test state is $7.9(1.5) \times 10^{-3}\,\mu{\rm s}^{-1}$, while the decay rate of the DFS state is $2.2(0.3) \times 10^{-3} \mu{\rm s}^{-1}$. The long lifetime of the DFS

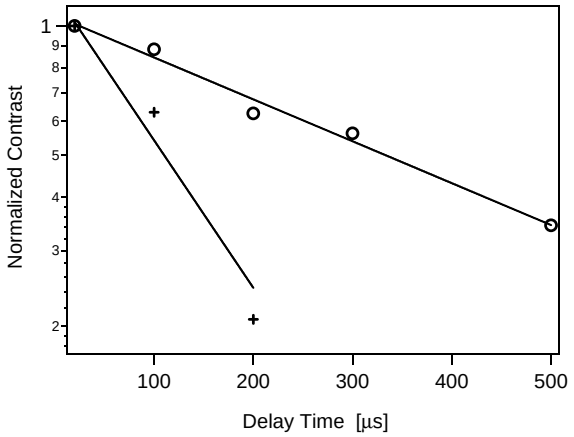

FIG. 6. Decay of DFS-encoded state (circles) and test state (crosses) under ambient decoherence. We vary the delay time between encoding and decoding to give the ambient noise a variable time to act. Coherence data are normalized to their values for zero delay time. The fit lines are exponential decay curves for purposes of comparison and are not theoretical predictions.

state shows that collective dephasing from magnetic field noise is the major ambient source of decoherence for the test state. The loss of coherence of the encoded state is consistent with degradation of the decoding pulses [2,31] due to heating of the ion motional state over the delay time [17].

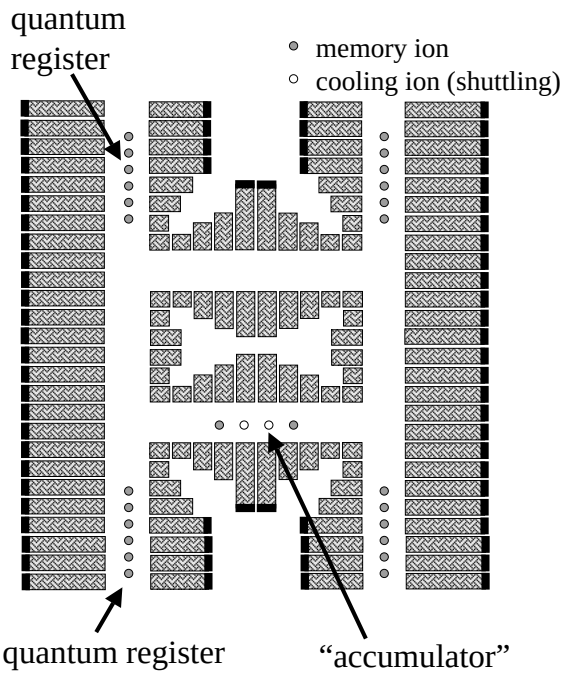

FIG. 7. Schematic of the proposed “quantum CCD” architecture for a large-scale ion-trap quantum computer. The “logic ions”, which encode the quantum information, are held in a storage region. To perform a logic operation, we shuttle the relevant logic ions into the “accumulator” region, where they interact with lasers. Auxiliary “cooling ions” are provided for sympathetic cooling of the logic ions, which will almost certainly heat up during transfer to the accumulator.

V. CONCLUSION AND OUTLOOK

We have demonstrated four-particle entanglement, violation of Bell’s inequality, and encoding into a decoherence-free subspace using a small quantum register of trapped ions. While these experiments are important steps on the road to quantum computation, the major challenge remains: scaling up the techniques developed for a few ions to build a large-scale quantum computer with thousands or millions of qubits. Fortunately, we have a plausible roadmap to our goal, the “quantum CCD” model of ion-trap quantum computing (Fig. 7). We envision a large ion trap with many independent DC electrodes, which could be used to move ions between storage regions and “accumulator” regions in which quantum logic operations take place. Such a trap could hold thousands of ions, but avoids the slow gate speeds and detection inefficiency associated with large ion crystals by allowing us to work with only a few qubits at a time. Though the ions would most likely heat up while being moved around, the addition of another ion species would enable us to sympathetically cool the ions before performing logic [32]. The DFS encoding demonstrated above would permit us to move qubits around without incurring dephasing from the spatial variation of magnetic fields across the device. In pursuit of the “quantum CCD” goal, we have built a trap supporting a double-well potential with spacing about 1 mm and plan to explore ways of maintaining quantum coherence and entanglement over these large distances.

ACKNOWLEDGMENTS

This research was supported by the NSA, ARDA, ARO, and ONR. This paper is a contribution of the National Institute of Standards and Technology and is not subject to U.S. copyright.

[1] C.A. Sackett, D. Kielpinski, B.E. King, C. Langer, V. Meyer, C.J. Myatt, M. Rowe, Q.A. Turchette, W.M. Itano, D.J. Wineland, and C. Monroe, Nature 404, 256 (2000).

[2] A. Sørensen and K. Mølmer, *Phys. Rev. Lett.* 82, 1971 (1999); K. Mølmer and A. Sørensen, *Phys. Rev. Lett.* 82, 1835 (1999); E. Solano, R.L. de Matos Filho, and N. Zagury, *Phys. Rev. A* **59**, 2539 (1999); A. Sørensen and K. Mølmer, *Phys. Rev. A* 62, 022311 (2000).

[3] M.A. Rowe, D. Kielpinski, V. Meyer, C.A. Sackett, W.M. Itano, C. Monroe, and D.J. Wineland, *Nature* **409**, 791 (2001).

[4] D. Kielpinski, V. Meyer, M.A. Rowe, C.A. Sackett, W.M. Itano, C. Monroe, and D.J. Wineland, *Science* **291**, 1013 (2001).

[5] P.W. Shor, in *Proc. 35th Ann. Symp. on Found. Comp. Sci.*, S. Goldwasser, Ed. (IEEE Computer Society, Los Alamitos, CA, 1994), p. 116.

[6] L.K. Grover, *Phys. Rev. Lett.* **79**, 325 (1997).

[7] F. Diedrich, J.C. Bergquist, W.M. Itano, and D.J. Wineland, *Phys. Rev. Lett.* **62**, 403 (1989).

[8] B.E. King, C.S. Wood, C.J. Myatt, Q.A. Turchette, D. Leibfried, W.M. Itano, C. Monroe, and D.J. Wineland, *Phys. Rev. Lett.* **81**, 1525 (1998).

[9] This requirement can be relaxed further in some cases, as pointed out by W. Dür and J.I. Cirac (quant-ph/0011025).

[10] C. Roos, T. Zeiger, H. Rohde, H.C. Ngerl, J. Eschner, D. Leibfried, F. Schmidt-Kaler, and R. Blatt, *Phys. Rev. Lett.* **83**, 4713 (1999).

[11] W.M. Itano, J.C. Bergquist, J.J. Bollinger, J.M. Gilligan, D.J. Heinzen, F.L. Moore, M.G. Raizen, and D.J. Wineland, *Phys. Rev. A* **47**, 3554 (1993).

[12] P.T.H. Fisk, *Rep. Prog. Phys.* **60**, 761 (1997).

[13] F. Schmidt-Kaler, C. Roos, H.C. Nagerl, H. Rohde, S. Gulde, A. Mundt, M. Lederbauer, G. Thalhammer, T. Zeiger, P. Barton, L. Hornekaer, G. Reymond, D. Leibfried, J. Eschner, and R. Blatt, *J. Mod. Opt.* **47**, 2573 (2000).

[14] C. Monroe, D.M. Meekhof, B.E. King, W.M. Itano, and D.J. Wineland, *Phys. Rev. Lett.* **75**, 4714 (1995).

[15] H.C. Nägerl, D. Leibfried, H. Rohde, G. Thalhammer, J. Eschner, F. Schmidt-Kaler, and R. Blatt, *Phys. Rev. A* **60**, 145 (1999).

[16] M.G. Raizen, J.M. Gilligan, J.C. Bergquist, W.M. Itano, and D.J. Wineland, *J. Mod. Opt.* **39**, 233 (1992).

[17] Q. A. Turchette, D. Kielpinski, B.E. King, D. Leibfried, D.M. Meekhof, C.J. Myatt, M.A. Rowe, C.A. Sackett, C.S. Wood, W.M. Itano, C. Monroe, and D.J. Wineland, *Phys. Rev. A* **61**, 063418 (2000).

[18] A. Einstein, B. Podolsky, and N. Rosen, *Phys. Rev.* **47**, 777 (1935).

[19] J.S. Bell, *Physics* (N.Y.) **1**, 195 (1965).

[20] J.F. Clauser, M.A. Horne, A. Shimony, and R.A. Holt, *Phys. Rev. Lett.* **23**, 880 (1969).

[21] M. Lamehi-Rachti and W. Mittig, *Phys. Rev. D* **14**, 2543 (1976).

[22] A. Garg and N.D. Mermin, *Phys. Rev. D* **35**, 3831 (1987), and references therein.

[23] A. Aspect, *Nature* **398**, 189 (1999).

[24] W.H. Zurek, *Phys. Today* **44**, 36 (1991).

[25] D. Giulini, E. Joos, C. Kiefer, J. Kupsch, I.-O. Stamatescu, H.D. Zeh, *Decoherence and the Appearance of a Classical World in Quantum Theory* (Springer, Berlin, 1996).

[26] *Fortsch. der Physik* **46**, No. 4-8 (1998).

[27] *Fortsch. der Physik* **48**, No. 9-11 (2000).

[28] D.A. Lidar, I. L. Chuang, and K. B. Whaley, *Phys. Rev. Lett.* **81**, 2594 (1998).

[29] P. Zanardi and M. Rasetti, *Phys. Rev. Lett.* **79**, 3306 (1997).

[30] L.M. Duan and G.C. Guo, *Phys. Rev. A* **57**, 737 (1998).

[31] D.J. Wineland, C. Monroe, W.M. Itano, D. Leibfried, B.E. King, and D.M. Meekhof, *J. Res. NIST* **103**, 259 (1998).

[32] D. Kielpinski, B.E. King, C.J. Myatt, C.A. Sackett, Q.A. Turchette, W.M. Itano, C. Monroe, D.J. Wineland, and W.H. Zurek, *Phys. Rev. A* **61**, 032310 (2000).